Thioredoxin1 is a target to attenuate diabetes-induced RPE cell dysfunction in human ARPE19 cells by alleviating oxidative stress

HUI QI[1*], TIANHE LIU[1*], JIASU LIU[1,2], QIUFENG TENG[1], ZHONGPING MA[1], SHENGNAN WANG[1], SHIHUI WEN[1], CHENGHONG ZHANG[1], XIANG REN[1], HUI KONG[2] and LI KONG[1]

[1]Department of Histology and Embryology, College of Basic Medicine, Dalian Medical University, Dalian, Liaoning 116044; [2]Department of Otorhinolaryngology, The Second Hospital, Dalian Medical University, Dalian, Liaoning 116023, P.R. China

Received January 28, 2023; Accepted April 25, 2023

DOI: 10.3892/mmr.2023.13021

Abstract. Diabetes-induced cell dysfunction of the retinal pigment epithelium (RPE) contributes to the initiation and progression of diabetic retinopathy (DR). Thioredoxin 1 (Trx1) plays a key role in DR. However, the effect and mechanism of Trx1 on diabetes-induced cell dysfunction of the RPE is not fully understood during DR. In the present study, the effect of Trx1 on this process and its related mechanism were investigated. A Trx1 overexpression cell line, ARPE19-Trx1/LacZ, was constructed and treated with or without high glucose (HG). Flow cytometry was used to analyze apoptosis of these cells and the mitochondrial membrane potential was analyzed using JC-1 staining solution. A DCFH-DA probe was also used to detect the reactive oxygen species (ROS) generation. Western blotting was used to examine the expression of related proteins in ARPE-19 cells after HG treatment. The results demonstrated that the RPE layer was damaged in clinical samples. ROS formation and RPE cell dysfunction increased after HG treatment *in vitro*. Besides, the expression of mitochondrial-mediated apoptosis related proteins (Bax, apoptosis-inducing factor, cytochrome C, Caspase3 and Caspase9) also increased; however, overexpression of Trx1 attenuated these changes and improved the function of ARPE19 cells. These results indicated that overexpression of Trx1 alleviated diabetes-induced RPE cell dysfunction in DR by attenuating oxidative stress.

Correspondence to: Professor Li Kong, Department of Histology and Embryology, College of Basic Medicine, Dalian Medical University, 9 West Section Lvshun South Road, Dalian, Liaoning 116044, P.R. China
E-mail: kongli@dmu.edu.cn

Professor Hui Kong, Department of Otorhinolaryngology, The Second Hospital, Dalian Medical University, 467 Zhongshan Road, Dalian, Liaoning 116023, P.R. China
E-mail: konghui@dmu.edu.cn

*Contributed equally

Key words: diabetic retinopathy, retinal pigment epithelium, thioredoxin1, oxidative stress, apoptosis

Introduction

Diabetic retinopathy (DR) is one of the most serious complications of diabetes mellitus. DR is the primary cause of vision impairment and blindness in patients with diabetes worldwide (1). In recent years, it has been demonstrated that retinal neurodegeneration is found in patients with diabetes (2) and is involved in the initiation and progression of DR (3); however, the effects of diabetes on the retinal pigment epithelium (RPE) have received markedly less attention (4). The RPE is a monolayer of pigmented cells located between the neuroretina and choroids. Cells of the RPE have many biological functions including transporting nutrients, ions, water and metabolic end products. Cells of the RPE are also involved in renewing photoreceptor outer segments, which affect vision and form the outer blood-retina barrier. Dysfunction of the cells in the RPE has been reported in numerous inherited and acquired diseases that cause permanent blindness (5). More specifically, the breakdown of the RPE barrier is associated with DR (6), and RPE cell dysfunction plays important roles in DR physiopathology (7). Besides, RPE treated with glucose is commonly used as an ideal *in vitro* model for DR research (8).

The main pathophysiology of DR is various changes caused by hyperglycemia, which can induce multiple factors and signaling pathways involved in processes such as oxidative stress (OS) and autophagy (9). OS is a phenomenon caused by an imbalance between reactive oxygen species (ROS) production and the antioxidant system in cells and tissues. OS can lead to mitochondrial dysfunction which plays a critical role in the pathogenesis of DR. Certain studies have demonstrated that OS is involved in the course of DR (10,11). Therefore, inhibiting ROS generation or scavenging excessive ROS have been employed as therapeutic strategies for the treatment of DR (12).

The thioredoxin (Trx) antioxidant system consists of Trx, Trx reductases, NADPH and peroxiredoxin (13,14). Trx is the major component of the Trx antioxidant system. It acts as the natural barrier for cells in the defense of OS, anti-apoptosis (15) and regulating autophagy (16). There are three types of Trx:

Trx1 located in the cytoplasm, Trx2 located in the mitochondria and Trx3 located in sperm.

Extensive research has been reported on the pathophysiology of DR; however, the exact etiology of this disease is not fully understood, and little attention has been paid to the role of RPE in DR. Thus, ARPE19 cells were used to investigate the effect of Trx1 on high glucose (HG)-induced RPE cell dysfunction and its related mechanism *in vitro*, with the aim of finding and providing evidence for new clinical therapeutic targets of DR in the future.

Materials and methods

Patients. The present study included 100 patients with diabetes and 30 healthy individuals as the control group. All patients (mean age, 63 years; male/female ratio, 1:1) were recruited (from January 2020 to January 2021) from the Department of Endocrinology at The Second Hospital of Dalian Medical University (Dalian, China). The patients with diabetes were divided into non-DR (NDR), non-proliferative DR (NPDR) and proliferative DR (PDR) groups. All participants underwent optical coherence tomography (OCT) and full-field Electroretinogram (ERG) on the same day. Signed consent forms were obtained from all patients. The present study was approved (approval no. 2020008; approval date, January 10, 2020) by the ethics committee of The Second Hospital of Dalian Medical University (Dalian, China).

Cell culture and treatment. The ARPE19 cell line was obtained from the Institute of Biochemistry and Cell Biology, Chinese Academy of Sciences and maintained in DMEM-F12 medium (Gibco; Thermo Fisher Scientific, Inc.) containing 10% fetal bovine serum (Biological Industries), penicillin (100 U/ml) and streptomycin (100 μg/ml) (HyClone; Cytiva). ARPE19-Trx1 and ARPE19-LacZ were either untreated or treated with 75 mM glucose and mannitol for 24 h in the experiment.

Measurement of intracellular ROS. The generation of intracellular ROS was detected by the DCFH-DA probe method (cat. no. S0033S; Beyotime Institute of Biotechnology). Briefly, the cells were seeded in 6-well plates at $2x10^5$ cells/well and all groups were treated with or without high glucose (75 mM) for 24 h. Cells were then washed with PBS three times, before incubating with a DCFH-DA probe at a final concentration of 10 μmol/l at 37˚C for 30 min. Fluorescence intensity was measured by a fluorescence microscope.

Measurement of mitochondrial membrane potential (MMP). Cells were seeded in a six-well plate (Guangzhou Jet Bio-Filtration Co., Ltd.) at a density of $2x10^5$ cells/well. Briefly, the cells in all groups were treated with or without high glucose (75 mM). After washing with PBS, the cells were incubated with 1 ml cell culture medium and 1 ml JC-1 staining solution (Beyotime Institute of Biotechnology) at 37˚C in a cell incubator for 20 min. Images were obtained using fluorescence microscopy (NikonTi-S; Nikon Corporation).

Western blotting. The cells were lysed on ice in buffer containing 50 mM Tris-HCl pH 8.0, 150 mM NaCl, 1% Nonidet P-40, 0.5% deoxycholate, 0.1% SDS, 1 mM PMSF and 150 U/ml aprotinin. The concentration of the protein was measured by BCA assay. The same amount of protein (30 μg/lane) was loaded on a 10% polyacrylamide gel for each sample. Proteins separated by SDS-PAGE were electro-transferred to PVDF membranes. The membranes were blocked with 5% skimmed milk diluted with TBST (0.5% Tween-20) at room temperature for 1.5 h and then incubated with the following primary antibodies: β-actin (Santa Cruz Biotechnology Inc.; cat. no. sc-47778; 1:1,000), cytochrome C (Cyt C; Abcam; cat. no. ab133504; 1:1,000), Bax (Proteintech Group, Inc.; cat. no. 50599-2-Ig; 1:1,000), Bcl-2 (Abcam; cat. no. ab182858; 1:1,000), apoptosis-inducing factor (AIF; Abcam; cat. no. ab1998; 1:1,000), Trx1 (Abcam; cat. no. ab133524; 1:5,000), RPE65 (Abcam; cat. no. ab231782; 1:1,000), Caspase9 (Proteintech Group, Inc.; cat. no. 10380-1-AP; 1:1,000), Caspase3 (Proteintech Group, Inc.; cat. no. 19677-1-AP; 1:1,000) and zonula occludens-1 (ZO-1; Proteintech Group, Inc.; cat. no. 21773-1-AP; 1:1,000), overnight at 4˚C. Membranes were washed with TTBS three times for 10 min each and incubated with the appropriate secondary antibody (goat anti-rabbit IgG; cat. no. SA00001-2; or goat anti-mouse IgG; cat. no. SA00001-1; both Proteintech Group, Inc.) diluted in blocking buffer at 1:1,000, for 1 h at room temperature. Protein bands were imaged using the enhanced chemiluminescence system (Bio-Rad Laboratories, Inc.). The intensities of the bands were measured using the LabWorks 4.5 software (Analytik Jena AG).

Generation of stable cell line. The recombinant plasmids (0.4 μg) (16), pIRES2-EGFP-Trx1 and pIRES2-EGFP-LacZ, were transfected into ARPE19 cells using the Effectene Transfection Reagent (Qiagen China Co.) according to the manufacturer's protocol. Transfection complexes were removed and fresh medium was added to the cells. The cells were then incubated in their normal growth conditions after transfection at 37˚C for 24 h. A fluorescent microscope was used to check for transfection efficiency. Stable cell lines were prepared by selection in medium containing 500 μg/ml G418 (Sigma-Aldrich; Merck KGaA). After 4 weeks of selection, several independent clones were picked and were confirmed by immunofluorescence or western blotting to detect the target protein level expression.

Immunofluorescence. The cells were seeded onto coverslips, followed by treatment when the cells reached ~80% confluency. The medium was removed and the cells were washed twice with PBS. The cells were then fixed in 4% paraformaldehyde at room temperature for 30 min, followed by incubation with PBS containing 0.25% Triton X-100 (Sigma-Aldrich; Merck KGaA) for 10 min. The cells were washed in PBST (containing 0.025% Tween) three times for 5 min, and then blocked with 10% normal horse serum (Beijing Solarbio Science & Technology Co., Ltd.) in PBST (containing 0.1% Tween) for 1 h. Lastly, slides were incubated with ZO-1 primary antibody (Proteintech Group, Inc.; cat. no. 21773-1-AP; 1:500), Trx1 (Abcam; cat. no. ab133524;

1:100) at 4˚C overnight. The cells were then washed with PBST three times, followed by incubation with secondary antibody (Invitrogen; Thermo Fisher Scientific, Inc.; cat. no. A16111/A-31572; 1:2,000) diluted in blocking buffer at room temperature for 1 h in the dark. DAPI (0.9 μg/ml) was also used to stain the nucleus. One drop of mounting medium (cat. no. H-1000; Vector Laboratories, Inc.) was loaded on top of the specimen, before coverslips were placed on the slides. Fluorescence images were acquired by a fluorescent microscope (NikonTi-S; Nikon Corporation).

Flow cytometric analysis. Cell apoptosis was analyzed by staining with Annexin V/propidium iodide (PI) (Nanjing KeyGen Biotech Co., Ltd.). Briefly, ARPE19 cells were treated with HG for 24 h. The cells were washed twice with PBS and resuspended in 500 μl 1X binding buffer (Nanjing KeyGen Biotech Co., Ltd.), followed by incubation at 25˚C for 15 min in the dark. Fluorescence of PI and Annexin V was monitored by FACS (ACEA Bio-science, Inc.) at 525 and 630 nm, respectively. The data was analyzed using BD Accuri C6 software (BD Biosciences).

Trans-epithelial electrical resistance (TEER) measurement. ARPE19 cells ($5x10^4$ cells/well) were cultured in Transwell inserts on a 0.4-μm pore polyethylene terephthalate membrane (6.5 mm diameter; Corning Inc.). The media were replaced every 2-3 days after the cells adhered to the membrane. TEER was conducted over a 4-week period using an EVOM 2 epithelial volt ohmmeter and 4-mm STX2 chopstick electrode (World Precision Instruments). Briefly, the electrode was sterilized in 70% ethanol, rinsed in PBS and equilibrated in pre-warmed culture medium before being placed into the apical and basal Transwell compartments. Measurements were recorded from at least five separate wells per experiment. In each well, three measurements were recorded to obtain an average value. The TEER value was calculated using the following formula: TEER (Ω cm^2)=[total resistance-blank resistance (Ω)]x[area (cm^2)].

Transmission electron microscopy (TEM). The ARPE19 cells were treated with different experimental conditions, collected and fixed at 4˚C with glutaraldehyde. PBS (0.1 M) was used to wash the samples three times for 15 min each time, and then the samples were stained with osmic anhydride at room temperature for 2 h. The samples were washed again with 0.1 M PBS three times for 15 min each, and then dehydrated using an ethanol series. Epoxy propylene was used for 10 min and the sample was placed into Epon12 embedding medium (GP18010). Next, the samples were heated in a 37˚C oven for 24 h, a 45˚C oven for 24 h and a 60˚C oven for 48 h. Ultrathin slices were prepared and observed under a transmission electron microscope (JEM-2000EX; JEOL Ltd.).

Detection of SOD activity. ARPE19 cells ($3x10^5$ cells/well) were seeded in six-well plates. Then cells were treated with 75 mM glucose for 24 h when the cell confluence reached 50-60%. The SOD activity in ARPE19 cells was detected by the kit provided by the Beyotime Institute of Biotechnology (cat. no. S0101S), according to the manufacturer's instructions. The intracellular SOD activity was detected by microplate reader at a wavelength of 450 nm.

Statistical analysis. The data were presented as the mean ± SD from three independent experiments and analyzed by unpaired Student's t-test (two groups) or one-way ANOVA (three or more groups) followed by Tukey's or Bonferroni's post hoc test. All statistical analyses were conducted using GraphPad Prism (version 6.0; Dotmatics). $P<0.05$ was considered to indicate a statistically significant difference.

Results

Diabetes-induced RPE cell degeneration with vision damage in clinical patients. Aiming to explore the association of DR with RPE cells, data of clinical patients were collected. As shown in the OCT images in Fig. 1, there was no difference in the morphology of the RPE layer in patients with diabetes in the NDR group compared with the control group; however, the OCT images of the NPDR and PDR groups exhibited an abnormal morphology of the RPE layer compared with the control group. Moreover, the ERG results for the patients with diabetes in the NDR, NPDR and PDR groups demonstrated that the A-wave and B-wave amplitudes of the rods and cones were decreased compared with the control group.

Diabetes-induced RPE cell apoptosis in vitro. Aiming to explore the effect of glucose-induced high osmotic pressure as well as HG in RPE cell, a cell viability experiment was performed using mannitol (equal concentration to the HG) to explore the effect of osmotic pressure and no effect was observed (Fig. S1). In vitro cell apoptosis was analyzed by flow cytometry. As shown in Fig. 2A and B, the percentage of apoptotic cells increased significantly after HG treatment. The expression of the pro-apoptotic and anti-apoptotic proteins, Bax and Bcl-2, were also detected by western blotting. As demonstrated in Fig. 2C-E, the expression of Bax and Bcl-2 increased and decreased, respectively, after HG treatment, compared with the control group. In addition, the expression of Trx1 and RPE65 also decreased (Fig. 2C, F and G).

Overexpression of Trx1 attenuates diabetes-induced RPE cell apoptosis in vitro. After overexpression of Trx1 and the ARPE19-LacZ cells as the control, the apoptosis of ARPE19 cells was analyzed by flow cytometry. The stable overexpression Trx1 ARPE19 cell was identified by immunofluorescence and western blotting (Fig. 3A and B). As shown in Fig. 3C and D, the percentage of apoptotic cells increased in the ARPE19-LacZ cells after HG treatment whereas it decreased in the ARPE19-Trx1 cells. Additionally, the MMP assay results demonstrated that the red/green fluorescence ratio was decreased in the ARPE19 cells after HG treatment; however, this was reversed by overexpression of Trx1 (Fig. 3E and F).

Overexpression of Trx1 attenuates hyperglycemia-induced RPE cell dysfunction in vitro. The TEER and the expression of RPE65 and ZO-1 were measured to present the function of RPE cells after HG treatment *in vitro*. After HG treatment for 24 h, the TEER was decreased significantly both in the ARPE19-Trx1 and ARPE19-LacZ groups; however, the change was slow in the ARPE19-Trx1 group compared with the ARPE19-LacZ group (Fig. 4A). The expression of Trx1, RPE65 and ZO-1 decreased in the APRE19-LacZ group after

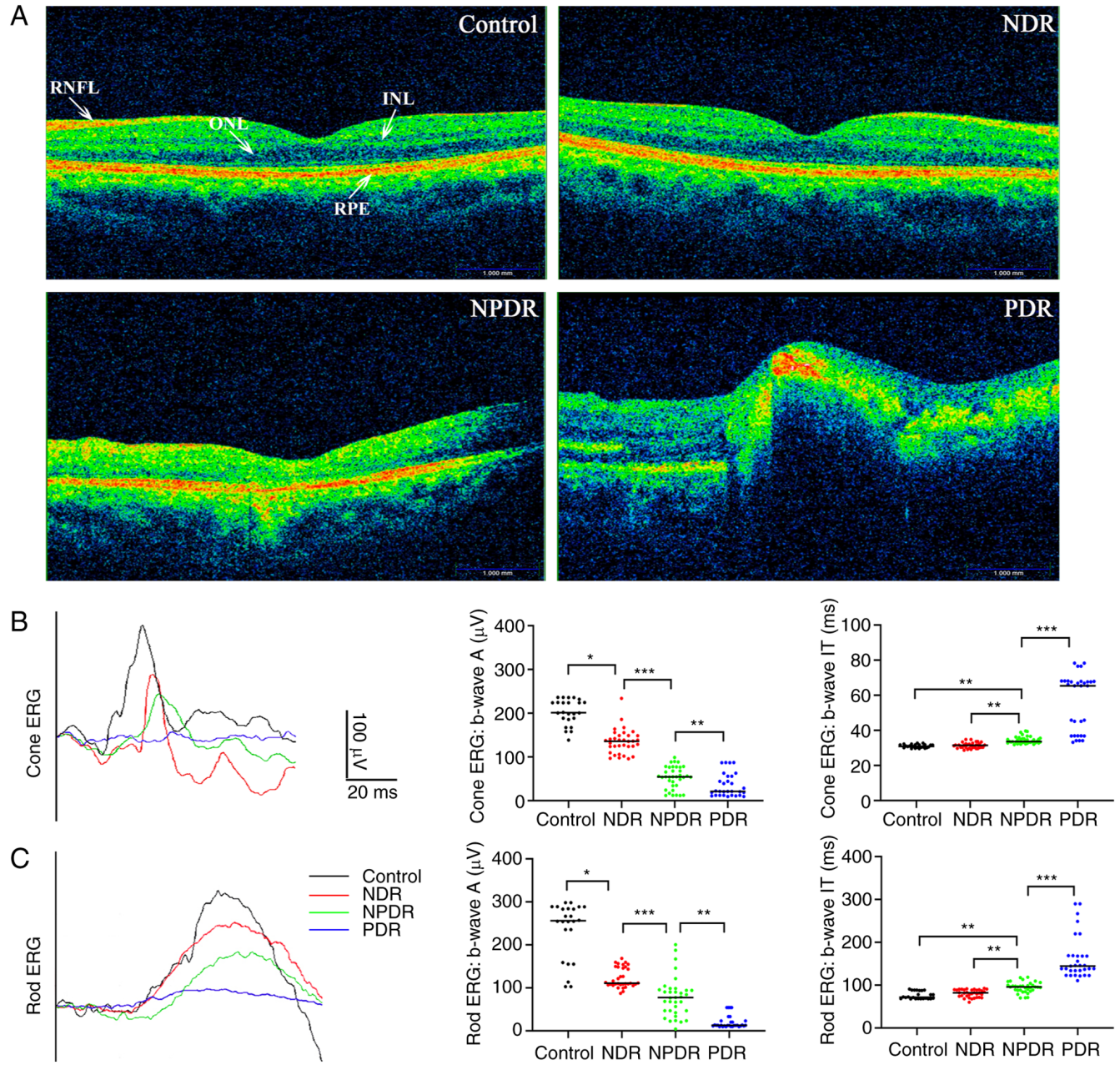

Figure 1. Diabetes-induced retinal pigment epithelium cell degeneration with vision damage in clinical patients. (A) Morphological changes in the retina of diabetic patients in the NDR, NPDR and PDR groups (100 patients with diabetes and 30 healthy individuals in the control group) were detected by optical coherence tomography. ERG A-wave and B-wave amplitudes of (B) cones and (C) rods of diabetic patients in the NDR, NPDR and PDR groups. The data are presented as the mean ± SD. *P<0.05, **P<0.01 and ***P<0.001. NDR, non-diabetic retinopathy; NPDR, non-proliferative diabetic retinopathy; PDR, proliferative diabetic retinopathy.

HG treatment; however, they increased in the APRE19-Trx1 group compared with APRE19-LacZ group (Fig. 4B-E). Besides, the immunofluorescent staining for the tight junction protein, ZO-1, demonstrated that the expression of continuous junctions between cells in the ARPE19-LacZ + HG group was decreased compared with the ARPE19-LacZ group, while it increased after Trx1 overexpression (Fig. 4F).

Overexpression of Trx1 attenuates hyperglycemia-induced RPE cell dysfunction via the OS/mitochondrial-mediated cell apoptotic pathway in vitro. As demonstrated in Fig. 5A and B, HG induced an increase in ROS formation; however, overexpression of Trx1 in ARPE19 cells attenuated the process. Furthermore, SOD activity was also detected to evaluate the level of OS (Fig. 5C). TEM was used to observe the effect of Trx1 overexpression on mitochondrial morphology in ARPE19 cells with or without HG treatment. The results demonstrated that the mitochondrial shape was abnormal and the membrane outline was unclear in ARPE19-LacZ cells compared with the ARPE19-Trx1 cells after HG treatment (Fig. 5D).

Moreover, western blotting was conducted to detect the expression of mitochondrial-mediated cell apoptotic proteins. The expression of Bax, AIF, cleaved-Caspase9, cleaved-Caspase3 and Cyt C increased in ARPE19-LacZ cells after HG treatment; however, the expression of Bcl-2 decreased. Overexpression of Trx1 downregulated the expression of Bax,

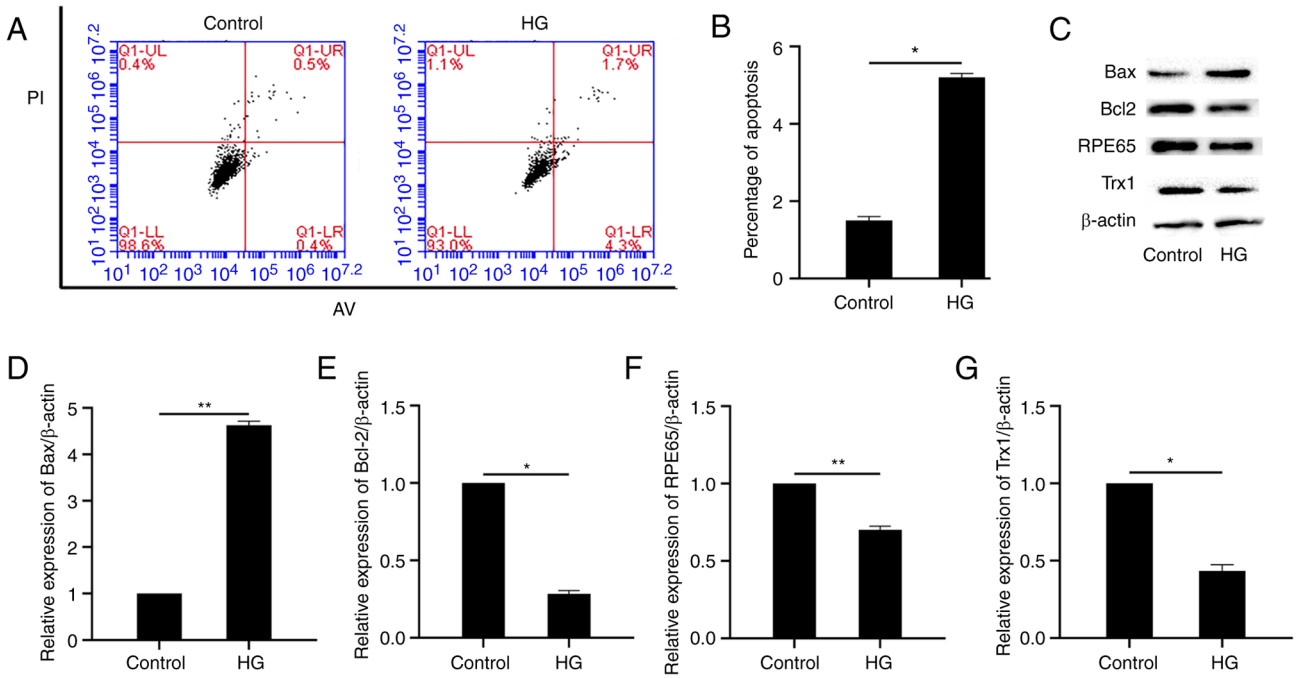

Figure 2. Diabetes-induced retinal pigment epithelium cell apoptosis *in vitro*. (A and B) Cell apoptosis was analyzed by flow cytometry after HG treatment. (C-G) The expression levels of (C and D) Bax, (C and E) Bcl-2, (C and F) RPE65 and (C and G) Trx1 in ARPE19 cells after HG treatment were detected by western blotting. The data are presented as the mean ± SD; n=3. *P<0.05 and **P<0.01. HG, high glucose; Trx1, thioredoxin1.

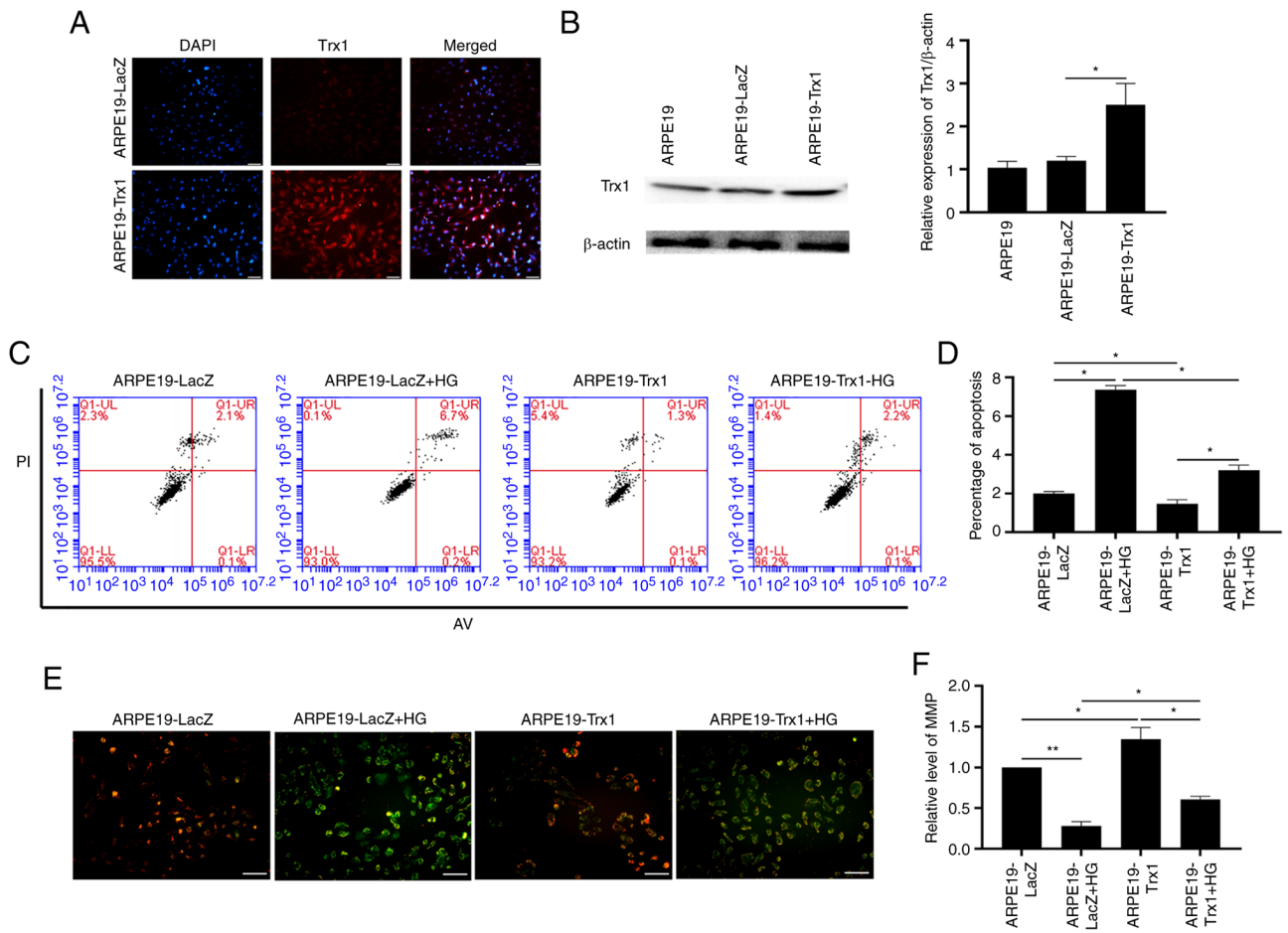

Figure 3. Overexpression of Trx1 attenuates diabetes-induced retinal pigment epithelium cell apoptosis *in vitro*. (A and B) The identification of stable overexpression Trx1 in ARPE19 cell was detected by immunofluorescence and western blotting. (C and D) The effect of Trx1 overexpression on the percentage of apoptotic ARPE19 cells with or without HG treatment. (E and F) The effect of Trx1 overexpression on mitochondrial membrane potential in ARPE19 cells with or without HG treatment (scale bar, 50 μm). Data are presented as the mean ± SD; n=3. *P<0.05 and **P<0.01. HG, high glucose; Trx1, thioredoxin1.

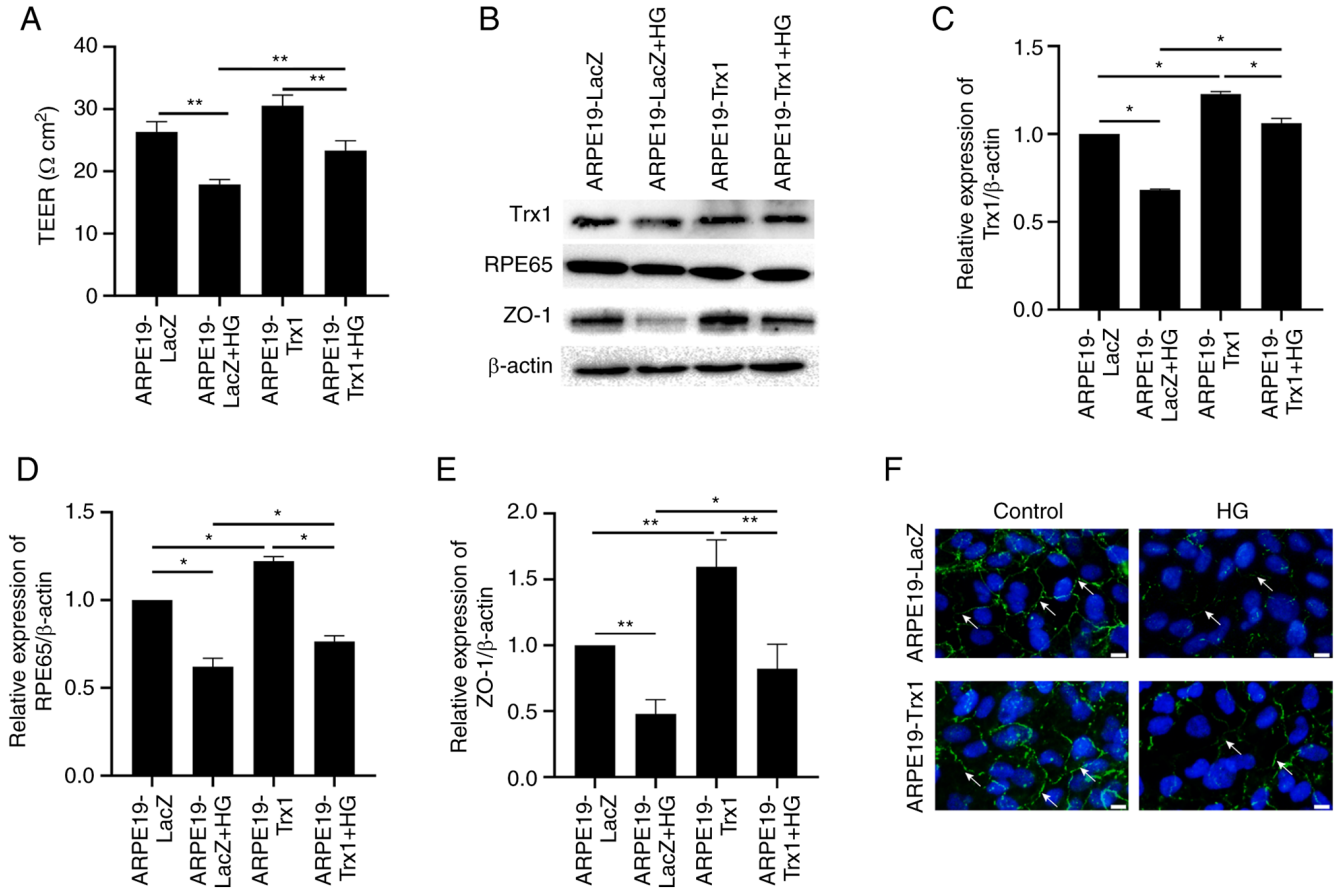

Figure 4. Overexpression of Trx1 delays diabetes-induced retinal pigment epithelium cell dysfunction *in vitro*. (A) Trans-epithelial electrical resistance values of ARPE19-Trx1/LacZ cells with or without HG treatment were measured at various times. (B) The expression of Trx1, RPE65 and ZO-1 in ARPE19-Trx1/LacZ cells with or without HG treatment were detected by western blotting. Semi-quantitative analysis of the expression of (C) Trx1, (D) RPE65 and (E) ZO-1 in ARPE19-Trx1/LacZ cells with or without HG treatment. (F) The expression of ZO-1 was detected by immunofluorescence staining in ARPE19-Trx1/LacZ cells with or without HG treatment (scale bar, 50 μm). Data are presented as the mean ± SD; n=3. *P<0.05 and **P<0.01. HG, high glucose; Trx1, thioredoxin1; ZO-1, zonula occludens-1.

AIF, cleaved-Caspase9, cleaved-Caspase3 and Cyt C, and upregulated the expression of Bcl-2 (Fig. 5E-K).

Discussion

DR is a leading cause of visual impairment and blindness in individuals aged 24-64 years old. Historically, DR was regarded as a common microvascular complication in diabetes. In the last few decades, most studies have focused on vascular abnormalities in DR. Diabetes-induced retinal vasculature abnormality was considered as the main cause of vision loss and impairment in patients with diabetes (17). Nevertheless, in recent years, alterations in the neural retina also have been detected, and their contribution to vision loss is under study (18). RPE cells are regarded as a component of the retina and play an important role in maintaining retina homeostasis, particularly in the maintenance of vision function; however, there are fewer studies reporting the role of RPE cells during DR. In the present study, it was found that hyperglycemia induced RPE cell damage *in vitro*, which was related to the downregulation of Trx1 expression. Moreover, hyperglycemia-induced RPE apoptosis in APRE19 cells was inhibited by Trx1 overexpression *in vitro*. These results indicated that Trx1 overexpression can inhibit ARPE19 cell apoptosis during DR *in vitro*.

The RPE cell has many functions, including active transport of ions and other substances, light absorption, photopigment renewal, trophic factor secretion, immune modulation and phagocytosis of the photoreceptor outer segment membranes (19,20); therefore, the function of ARPE19 cells in the presence or absence of HG treatment was analyzed in the present study. It was observed that the function of RPE cells decreased in the presence of HG treatment; however, overexpression of Trx1 reversed this process. These data suggested that hyperglycemia-induced RPE cell dysfunction was attenuated by overexpression of Trx1.

DR is the most common complication of diabetes, and the exact underlying mechanism is still not fully defined due to its multi-factorial character. Hyperglycemia, the condition that sustains abnormally HG levels in the blood, characterizes diabetes, and is considered to be involved in the initiation and progression of diabetes and its subsequent complications. Hyperglycemia affects the cells in multiple ways, including by non-enzymatic based protein modification, OS, chronic inflammation and the activation of the protein kinase C pathway (21-24). OS has been implicated in a host of diseases, including diabetes and its complications. In the present study, the main focus was on OS-induced apoptosis after HG treatment in ARPE19 cells. When

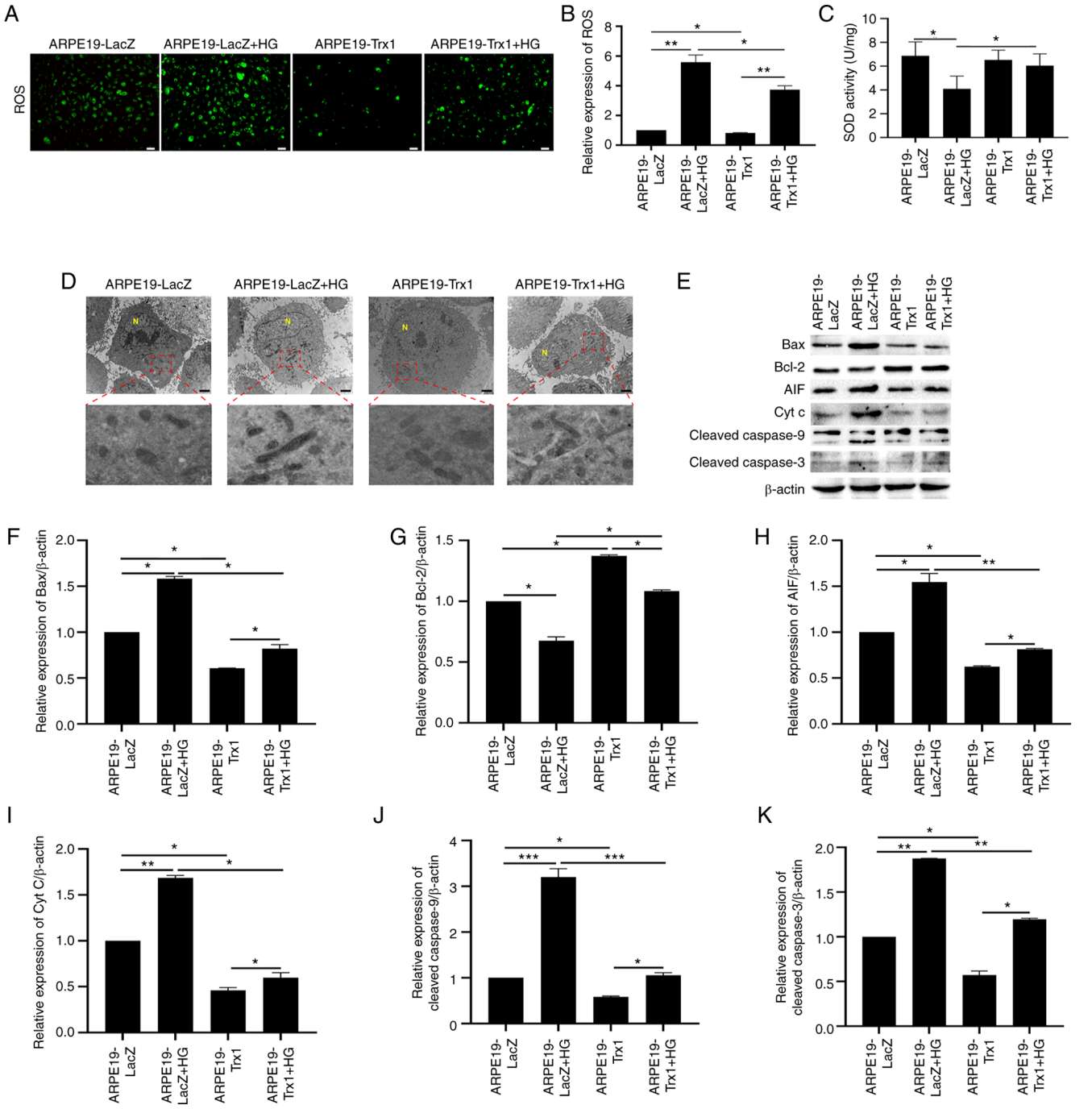

Figure 5. Overexpression of Trx1 delays diabetes-induced RPE cell dysfunction via the ROS/mitochondrial-mediated cell apoptotic pathway *in vitro*. (A and B) The effect of Trx1 overexpression on ROS generation in ARPE19 cells with or without HG treatment (scale bar, 50 μm). (C) The effect of Trx1 overexpression on SOD activity in ARPE19 cells with or without HG treatment. (D) The effect of Trx1 overexpression on mitochondrial morphology in ARPE19 cells after HG treatment (scale bar, 2 μm). (E) Representative western blotting images showing the effect of Trx1 overexpression on the expression of Bax, Bcl-2, AIF, Cyt C, cleaved-Caspase9 and cleaved-Caspase3 in ARPE19 cells with or without HG treatment. Semi-quantitative analysis showed the effect of Trx1 overexpression on the expression of (F) Bax, (G) Bcl-2, (H) AIF, (I) Cyt C, (J) cleaved-Caspase9 and (K) cleaved-Caspase3 in ARPE19 cells with or without HG treatment. β-actin was used as the internal control. Data are presented as the mean ± SD; n=3. *P<0.05, **P<0.01 and ***P<0.001. AIF, apoptosis-inducing factor; Cyt C, cytochrome C; HG, high glucose; N, nucleus; RPE, retinal pigment epithelium; ROS, reactive oxygen species; Trx1, thioredoxin1; SOD, superoxide dismutase.

ARPE19 cells were treated with HG, the formation of ROS increased significantly, the percentage of apoptotic ARPE19 cells increased and the MMP decreased. TEM was also used to observe the morphological changes of the mitochondria in ARPE19 cells after HG treatment. The morphology (shape and membrane) of mitochondria was abnormal after HG treatment. By contrast, the percentage of apoptotic cells decreased, the MMP increased and the morphology changes were markedly normal after Trx1 overexpression in ARPE19 cells, compared with the control group after HG treatment. In addition, the expression of mitochondrial-mediated cell apoptosis proteins was also detected to illustrate the related

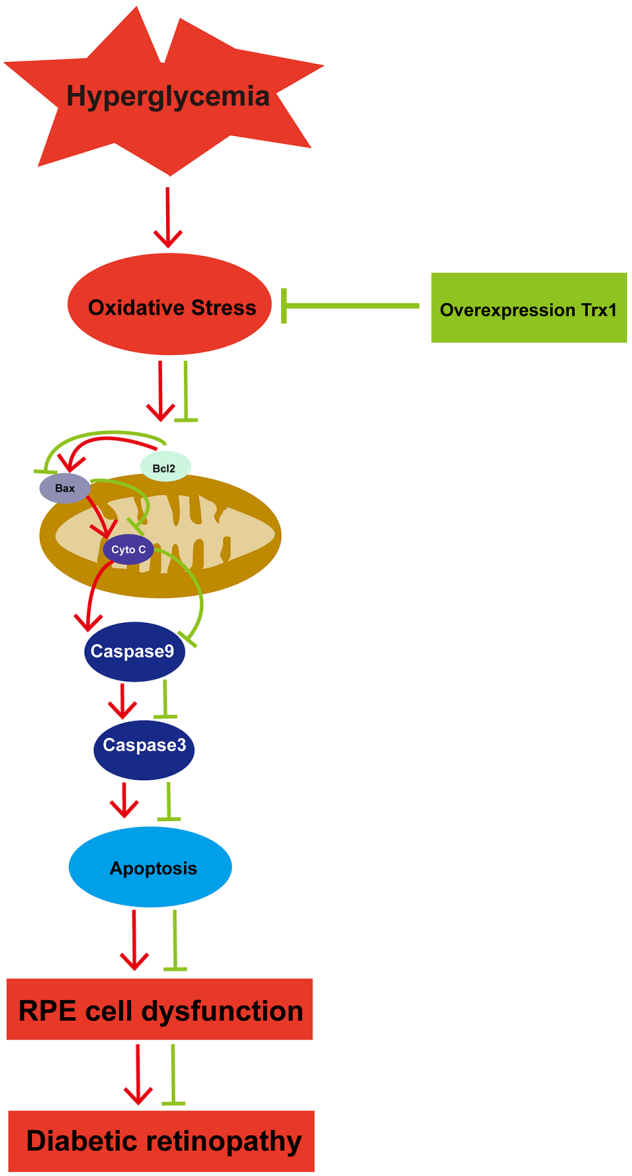

Figure 6. Summary of the effects and the related mechanism of Trx1 overexpression on diabetes-induced retinal pigment epithelium cell dysfunction in diabetic retinopathy. Trx1, thioredoxin1.

mechanism. In the present study, the expression of Bax, AIF, cleaved-Caspase9, cleaved-Caspase3 and Cyt C increased in ARPE19-LacZ cells after HG treatment; however, the expression of Bcl-2 decreased. Overexpression of Trx1 downregulated the expression of Bax, AIF, cleaved-Caspase9, cleaved-Caspase3 and Cyt C, and upregulated the expression of Bcl-2. These data suggested that Trx1 overexpression may protect ARPE19 cells from HG-induced dysfunction related to the ROS/mitochondrial-mediated cell apoptotic pathway. Autophagy is also closely related to DR, and a previous study also confirmed that autophagy plays an important role in DR (25). Piano *et al* (26) also observed increased autophagy levels in the other types of retina cells in STZ-induced diabetic mice, such as in the retinal ganglion cell layer. Nevertheless, there is a limitation to the present study; the ARPE19 cell line was only used as the model. In further research, it would be better to fully understand the mechanism by other cell lines or primary cell culture method together.

To summarize, it was demonstrated in the present study that overexpression of Trx1 could increase the function of ARPE19 cells and protected ARPE19 cells from hyperglycemia-induced cell dysfunction through regulating the ROS/mitochondria-mediated apoptosis pathway (Fig. 6). Furthermore, the relationship between thioredoxin1 and DR in clinic was also studied. Considering this, targeting Trx1 or its related signaling pathways may be a candidate therapeutic approach for the treatment or prevention of DR in the future.

Acknowledgements

Not applicable.

Funding

The present study was supported by The National Natural Science Foundation of China (grant no. 31371218) and The National and Local Joint Engineering Research Center for Mongolian Medicine Research and Development (grant no. MDK2019075). This project was also supported by The Liaoning Provincial Program for Top Discipline in Basic Medical Sciences and The Innovation and Entrepreneurship Training Program of Dalian Medical University (grant no. 2017161030).

Availability of data and materials

All data generated or analyzed during this study are included in this published article.

Authors' contributions

HQ, TL, JL, QT, ZM, CZ, SWa and SWe performed the experiments and interpreted the experimental results. HQ, XR, HK and LK conceived the idea and designed the experiments. TL, JL, QT, XR and ZM participated in the data analysis. XR and HQ wrote the manuscript. XR revised the manuscript. LK and HK funded the study. HK and LK confirm the authenticity of all the raw data. All authors read and approved the final manuscript.

Ethics approval and consent to participate

All participants were recruited from the Second Hospital of Dalian Medical University. The present study was approved (approval no. 2020008; approval date, January 10, 2020) by the ethics committee of The Second Hospital of Dalian Medical University (Dalian, China). Informed consent was obtained from all subjects involved in the study.

Patient consent for publication

Not applicable.

Competing interests

The authors declare that they have no competing interests.

References

1. Hendrick AM, Gibson MV and Kulshreshtha A: Diabetic retinopathy. Primary Care 42: 451-464, 2015.
2. Mrugacz M, Bryl A and Zorena K: Retinal vascular endothelial cell dysfunction and neuroretinal degeneration in diabetic patients. J Clin Med 10: 458, 2021.
3. Rossino MG, Dal Monte M and Casini G: Relationships between neurodegeneration and vascular damage in diabetic retinopathy. Front Neurosci 13: 1172, 2019.
4. Xia T and Rizzolo LJ: Effects of diabetic retinopathy on the barrier functions of the retinal pigment epithelium. Vision Res 139: 72-81, 2017.
5. Lakkaraju A, Umapathy A, Tan LX, Daniele L, Philp NJ, Boesze-Battaglia K and Williams DS: The cell biology of the retinal pigment epithelium. Prog Retin Eye Res: 100846, 2020. doi: 10.1016/j.preteyeres.2020.100846 (Epub ahead of print).
6. Simó R, Villarroel M, Corraliza L, Hernández C and Garcia-Ramírez M: The retinal pigment epithelium: Something more than a constituent of the blood-retinal barrier-implications for the pathogenesis of diabetic retinopathy. J Biomed Biotechnol 2010: 190724, 2010.
7. Tarchick MJ, Bassiri P, Rohwer RM and Samuels IS: Early functional and morphologic abnormalities in the diabetic nyxnob mouse retina. Invest Ophthalmol Vis Sci 57: 3496-3508, 2016.
8. Kim DI, Park MJ, Lim SK, Choi JH, Kim JC, Han HJ, Kundu TK, Park JI, Yoon KC, Park SW, *et al*: High-glucose-induced CARM1 expression regulates apoptosis of human retinal pigment epithelial cells via histone 3 arginine 17 dimethylation: Role in diabetic retinopathy. Arch Biochem Biophys 560: 36-43, 2014.
9. Dehdashtian E, Mehrzadi S, Yousefi B, Hosseinzadeh A, Reiter RJ, Safa M, Ghaznavi H and Naseripour M: Diabetic retinopathy pathogenesis and the ameliorating effects of melatonin; involvement of autophagy, inflammation and oxidative stress. Life Sci 193: 20-33, 2018.
10. Giacco F and Brownlee M: Oxidative stress and diabetic complications. Circ Res 107: 1058-1070, 2010.
11. Rodríguez ML, Pérez S, Mena-Mollá S, Desco MC and Ortega ÁL: Oxidative stress and microvascular alterations in diabetic retinopathy: Future therapies. Oxid Med Cell Longev 2019: 4940825, 2019.
12. Kang Q and Yang C: Oxidative stress and diabetic retinopathy: Molecular mechanisms, pathogenetic role and therapeutic implications. Redox Biol 37: 101799, 2020.
13. Yodoi J, Masutani H and Nakamura H: Redox regulation by the human thioredoxin system. Biofactors 15: 107-111, 2001.
14. Lu J and Holmgren A: The thioredoxin antioxidant system. Free Radical Biol Med 66: 75-87, 2014.
15. Zhang J, Li X, Han X, Liu R and Fang J: Targeting the Thioredoxin System for Cancer Therapy. Trends Pharmacol Sci 38: 794-808, 2017.
16. Ren X, Wang NN, Qi H, Qiu YY, Zhang CH, Brown E, Kong H and Kong L: Up-regulation thioredoxin inhibits advanced glycation end products-induced neurodegeneration. Cell Physiol Biochem 50: 1673-1686, 2018.
17. Tonade D and Kern TS: Photoreceptor cells and RPE contribute to the development of diabetic retinopathy. Prog Retin Eye Res 83: 100919, 2021.
18. Simó R, Stitt AW and Gardner TW: Neurodegeneration in diabetic retinopathy: Does it really matter? Diabetologia 61: 1902-1912, 2018.
19. Strauss O: The retinal pigment epithelium in visual function. Physiol Rev 85: 845-881, 2005.
20. Bonilha VL: Age and disease-related structural changes in the retinal pigment epithelium. Clin Ophthalmol 2: 413-424, 2008.
21. Nass N, Bartling B, Navarrete Santos A, Scheubel RJ, Börgermann J, Silber RE and Simm A: Advanced glycation end products, diabetes and ageing. Z Gerontol Geriatr 40: 349-356, 2007.
22. Volpe CMO, Villar-Delfino PH, Dos Anjos PMF and Nogueira-Machado JA: Cellular death, reactive oxygen species (ROS) and diabetic complications. Cell Death Dis 9: 119, 2018.
23. Koya D and King GL: Protein kinase C activation and the development of diabetic complications. Diabetes 47: 859-866, 1998.
24. Busik JV, Mohr S and Grant MB: Hyperglycemia-induced reactive oxygen species toxicity to endothelial cells is dependent on paracrine mediators. Diabetes 57: 1952-1965, 2008.
25. Fu D, Yu JY, Yang S, Wu M, Hammad SM, Connell AR, Du M, Chen J and Lyons TJ: Survival or death: A dual role for autophagy in stress-induced pericyte loss in diabetic retinopathy. Diabetologia 59: 2251-2261, 2016.
26. Piano I, Novelli E, Della Santina L, Strettoi E, Cervetto L and Gargini C: Involvement of autophagic pathway in the progression of retinal degeneration in a mouse model of diabetes. Front Cell Neurosci 10: 42, 2016.